Radar Reflection from Clouds: Gigahertz Backscatter Cross Sections and Doppler Spectra

David A. de Wolf, Herman W. J. Russchenberg, and Leo P. Ligthart

***Abstract*—This work deals with reflections of gigahertz-frequency radar signals from typical clouds over The Netherlands. Four principal mechanisms of reflection are identified. While the backscatter cross sections for these are mostly well known, there is a need to identify which, if any, are dominant in each frequency range. Numerical studies of superpositions of the main backscatter mechanisms are presented for a range of parameter values thought to occur commonly. These studies confirm previous results, but are generalized to incorporate gamma-function particle drop-size distributions. The results are relatively insensitive to the power of the diameter in the distribution function. The Doppler spectra of the reflected signals sometimes exhibit a bimodal form. One possible mechanism investigated here is the observation of reflections that occur simultaneously from turbulently moving globules of particles and from incoherent reflections from particles with diameter-dependent spreads in velocities.**

***Index Terms*—Clouds, doppler radar, radar cross section.**

I. Introduction

THE purpose of this study is to quantify and compare the diverse contributions to the radar backscatter cross section σ from clouds. Cloud altitudes and locations are such that contributions from ice particles are not expected to play a significant role. The major contributions come from distributions of liquid particles and possibly also from clear-air turbulence.

As there is a large and well-documented body of literature on the interaction of electromagnetic waves with various media, we give only a few key references to texts [1]–[3] for interactions with distributions of discrete particles [4], [5], with continuously varying random refractive-index media and [6], [7] specifically on applications to rain and clouds.The equations to be discussed and their backgrounds are to be found in the above references.

Fig. 1 depicts a typical radar backscatter experiment: a cloud particle at $\vec{r}_m$ is at distance R_m from the radar. The effective halfwidth of the radar beam is defined by angle θ and we assume quasi-monochromatic pulses centered around wavenumber k. The radar pulse defines a range cell of volume $v_{rc} \sim (R_m\theta)^2\ell$ around $\vec{r}_m$. Here, ℓ is the effective length of a range cell defined,

Manuscript received December 24, 1997; revised November 3, 1999.

D. A. de Wolf is with the Center for Stochastic Processes in Science and Engineering, Bradley Department of Electrical and Computer Engineering, Virginia Tech, Blacksburg, VA 24061-0111 USA.

H. W. J. Russchenberg and L. P. Ligthart are with the International Research Centre for Telecommunications-Transmission and Radar Faculty of Information Technology and Systems, Delft University of Technology, 2628 CD Delft, The Netherlands.

Publisher Item Identifier S 0018-926X(00)01653-7.

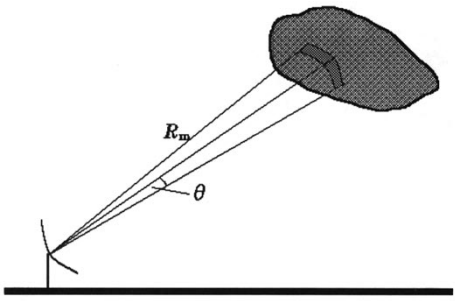

Fig. 1. Sketch of radar-cloud geometry.

for example, by the −10-dB power level of an individual pulse. Typical values for the 3.3-GHz DARR radar [8] are $\ell \approx 30$ m and $\theta \approx 0.9°$. If absorption of electromagnetic energy to and from a range cell is ignored, then the instantaneous radar backscatter cross section is defined as $\sigma(t) = 4\pi|f_{bs}|^2$ with

$$f_{bs}(t) = \sum_{m\epsilon v_{rc}} f_1(D_m)\, e^{2ikR_m(t)} \tag{1}$$

if $f_1(D_m)$ is the backscatter amplitude of a single particle at $\vec{r}_m$ with effective diameter D_m. It is reasonable to assume the Rayleigh backscatter cross section (which requires diameter $D \ll$ wavelength λ) for cloud particles at 1–10 GHz, i.e.,

$$f_1(D) = \frac{k^2D^3}{8}\,\frac{\varepsilon_r - 1}{\varepsilon_r + 2}. \tag{2}$$

Here, ε_r is the relative dielectric permittivity of the particle. In a continuum description, $D_m \rightarrow D$ and (1) is replaced by a spatially averaged quantity

$$f_{bs}(t) = \int_{v_{rc}} d^3r \int dD n_4(\vec{r}, D, t) f_1(D)\, e^{2ikR} \tag{3}$$

where $n_4(\vec{r}, D)\, dD$ represents the average number of particles per unit volume with diameters between D and $D + dD$. Experience with convection fogs [9] has shown that modified gamma functions are useful in modeling $n_4(\vec{r}, D, t)$

$$n_4(\vec{r}, D, t) = n_3(\vec{r}, t)\,\frac{q}{\Gamma\left(\dfrac{p+1}{q}\right)}\,\frac{1}{D_o}\left(\frac{D}{D_o}\right)^p \exp(-D/D_o)^q] \tag{4}$$

where $\Gamma(\cdots)$ is a gamma function, $n_3(\vec{r})$ is the usual particle density in m^{-3} and where q, p, and D_o also can be functions of

location and time, but will be assumed constant for convenience. Forms such as (4) are advantageous because (3) can then be written as

$$f_{bs}(t) = f_v \int_{v_{rc}} d^3r n_3(\vec{r}, t) \exp(2ikR) \quad \text{with}$$
$$f_v = \frac{q}{\Gamma\left(\frac{p+1}{q}\right)} \int_o^\infty dx x^p \exp(-x^q) f_1(D_o x) \quad (5)$$

which separates the statistics due to temporal variations in density from the individual particle-scattering amplitudes and the drop-size distribution in f_v. For narrow radar beams we replace kR by $\vec{k}\cdot\vec{R}$ with constant wavevector $\vec{k}$ in (5) when convenient. The coordinate origin is assumed at the radar location.

II. Rayleigh Scatterers

For Rayleigh-regime scatterers, it follows from (2) and (5) that

$$f_v = \frac{1}{8}\frac{\varepsilon_r - 1}{\varepsilon_r + 2} \frac{\Gamma\left(\frac{p+4}{q}\right)}{\Gamma\left(\frac{p+1}{q}\right)} k^2 D_o^3. \quad (6)$$

We now briefly review the backscatter cross sections for incoherent, coherent, quasi-coherent reflection, and for reflection from turbulence. There is a vast literature on most of these that we presume the reader to be familiar with.

A. Incoherent Reflection

Each particle is assumed to scatter independently of each other particle. Powers rather than amplitudes are added

$$\sigma_{inc} \equiv 4\pi\langle|f_{bs}|^2\rangle = 4\pi N|f_v|^2 = 4\pi\overline{n}_3 v_{rc}|f_v|^2 \quad (7)$$

given that N is the total number of particles and $\overline{n}_3$ is the mean particle density in the range cell with volume v_{rc}.

B. Coherent Reflection

All phase relationships between particles are assumed constant in time. The range cell volume can be written as $(R\theta)^2\ell$, where ℓ is an effective length of the range cell along the line of sight. It is assumed here that $\ell \ll R$. For a sufficiently short-range cell we obtain

$$f_{bs} = f_v\overline{n}_3(R\theta)^2 \int_{-\infty}^{\infty} dR s(R) \exp(2ikR)$$
$$= f_v\overline{n}_3(R\theta)^2 \tilde{s}(2k) \quad (8)$$

where $s(R)$ is an envelope function describing the radar range cell [e.g., a rectangular pulse of width ℓ or a Gaussian $\sim \exp(-R^2/\ell^2)$] and $\tilde{s}(2k)$ is its Fourier transform at wavenumber $2k$. We obtain

$$\sigma_{coh} = 4\pi|f_v|^2\overline{n}_3^2(R\theta)^4|\tilde{s}(2k)|^2. \quad (9)$$

Because $2k\ell \gg 1$ for the DARR or similar radars, it follows that $|\tilde{s}(2k)|^2 \ll 1$. The coherent cross section is usually negligibly small.

C. Quasi-Coherent Transport Reflection

The effect of density fluctuations due to transport of droplets by turbulent air ("passive additive") is considered. It follows from (5) that:

$$f_{bs} = f_v \int d^3r[\overline{n}_3(\vec{r}) + \delta n_3(\vec{r})]e^{2i\vec{k}\cdot\vec{R}}$$
$$= (f_{bs})_{coh} + \int d^3r\delta n_3(\vec{r})e^{2i\vec{k}\cdot\vec{R}} \quad (10)$$

so that a quasi-coherent contribution due to fluctuations in density is

$$\delta f_{bs} = \int d^3r\delta n_3(\vec{r})e^{2i\vec{k}\cdot\vec{R}}, \qquad \text{with} \quad \langle\delta f_{bs}\rangle = 0 \quad (11)$$

where $\langle\cdots\rangle$ indicates a mean value. The theory leading to a mean cross section is well understood [4]–[6], [13], [16], [17]. The wavenumber power spectrum of density fluctuations in the inertial subrange of turbulence is analogous to that for clear-air turbulence [4]

$$\Phi(K) \approx 0.033 C_{dens}^2 K^{-11/3} \approx 0.063\langle\delta n_3^2\rangle L_o^{-2/3} K^{-11/3} \quad (12)$$

in which expression L_o is the macroscale of turbulence. The factor 0.063 follows from the relationship between the refractive-index variance and the structure constant [5]: $\langle\delta n^2\rangle \approx 0.5234 C_n^2 L_o^{2/3}$. The passive-additive character of turbulence-carried droplets yields a similar relationship between $\langle\delta n_3^2\rangle$ and C_{dens}^2. One then obtains from (11) and (12):

$$\sigma_{qct} \approx 15.46 k^{-11/3} L_o^{-2/3} |f_v|^2 \int_{v_{rc}} d^3r_c\langle\delta n_3^2(\vec{r}_c)\rangle. \quad (13a)$$

The factor $15.46 = 0.063 \times 2^{4/3}\pi^4$. Under the assumption of uniform density in a range cell, this simplifies to

$$\sigma_{qct} \approx 15.46 k^{-11/3}\langle\delta n_3^2\rangle L_o^{-2/3}|f_v|^2 v_{rc} \quad (13b)$$

D. Quasi-Coherent Reflection Due to Clear-Air and Humidity Turbulence

The calculation for reflection from clear-air turbulence in the range cell follows the classical calculation of Booker and Gordon [13] based on the first Born approximation for the scattered field. It yields [13], [14],

$$\sigma_{qcah} \approx 8\pi^2 k^4 v_{rc}\Phi_n(2k) \approx 0.2052 v_{rc} C_n^2 k^{1/3} \quad (14)$$

where $\Phi_n(2k)$ is the power spectrum of refractive-index fluctuations due to temperature and humidity variations and C_n^2 is the structure constant. Gossard and Strauch [16] have previously concluded that this mechanism could be of importance, compared to incoherent scattering from clouds. Moreover, various authors [17], [18] point out that C_n^2 can be influenced significantly by fluctuations in the water-vapor density, so that numerical calculations of this parameter should take into account the fact that humidity fluctuations can be a major contributor (compared to clear-air density fluctuations).

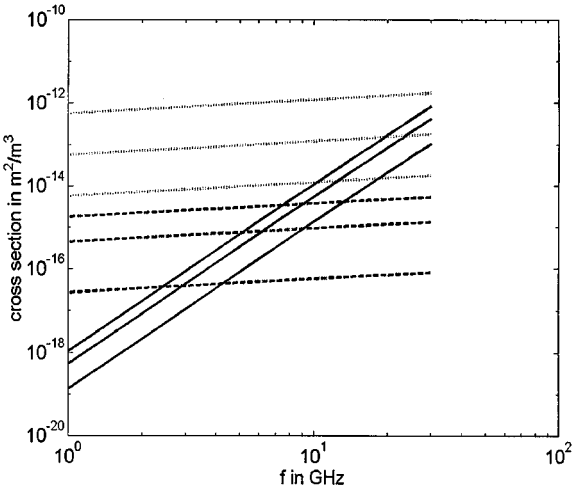

Fig. 2. Backscatter cross section as function of frequency [see (16)]: ___ $\sigma_{\rm inc}$ for $\overline{n}_3 = 100, 400$, and 800 particles per m^3, - - - σ_{qct} for $\sqrt{\langle \delta n_3^2 \rangle} = 100$, 400, and 800 particles per m^3, $\cdots$ σ_{qcah} for $C_n^2 = 10^{-14}$, 10^{-13}, and 10^{-12} in m$^{-2/3}$.

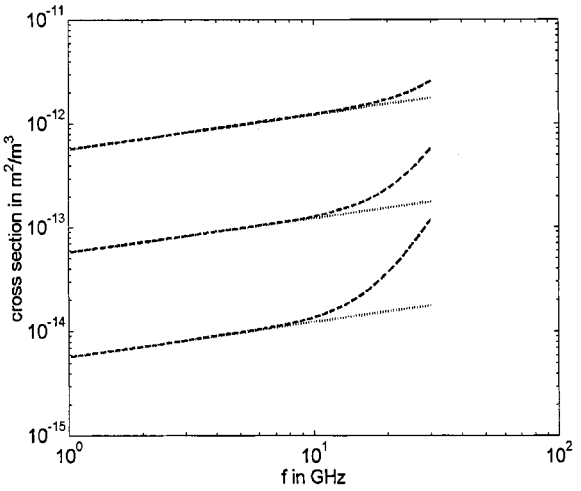

Fig. 3. Backscatter cross section as function of frequency [see (16)]: - - - $\sigma_{qct} + \sigma_{qcah}$, $\cdots$ $\sigma_{qct} + \sigma_{qcah} + \sigma_{inc}$ for $\overline{n}_3 = \sqrt{\langle \delta n_3^2 \rangle} = 100$ particles per m^3 and $C_n^2 = 10^{-14}$ in m$^{-2/3}$, $\overline{n}_3 = \sqrt{\langle \delta n_3^2 \rangle} = 400$ particles per m^3 and $C_n^2 = 10^{-13}$ in m$^{-2/3}$, $\overline{n}_3 = \sqrt{\langle \delta n_3^2 \rangle} = 800$ particles per m^3 and $C_n^2 = 10^{-12}$ in m$^{-2/3}$.

III. Some Numerical Comparisons

Consider some numerical values to see orders of magnitude of the various cross sections. It is common practice to choose $q = 1$ in (6). With that choice, it follows from (6) that $D_o = \overline{D}/(p+1)$ (if $\overline{D}$ is the mean drop diameter) and

$$|f_v|/k^2 = \frac{(p+3)(p+2)}{8(p+1)^2} \left| \frac{\varepsilon_r - 1}{\varepsilon_r + 2} \right| \overline{D}^3. \tag{15}$$

This factor has a weak dependence (compared to k^2) on frequency through ε_r. It is useful to separate it out in the expressions for the cross sections. The dependence upon p in (15) is also very weak for the usual range $4 < p < 6$. We shall choose $p = 5$. As a result

$$\begin{aligned} \sigma_{inc} &\approx 0.4751 \left| \frac{\varepsilon_r - 1}{\varepsilon_r + 2} \right|^2 \overline{n}_3 v_{rc} k^4 \overline{D}^6 \\ \sigma_{qct} &\approx 0.5845 \left| \frac{\varepsilon_r - 1}{\varepsilon_r + 2} \right|^2 \langle \delta n_3^2 \rangle v_{rc} k^{1/3} L_o^{-2/3} \overline{D}^6 \\ \sigma_{qcah} &\approx 0.2052 C_n^2 v_{rc} k^{1/3}. \end{aligned} \tag{16}$$

The range-cell volume is common to all three of these, hence, we will show cross sections per unit range-cell volume. Of the radar, only its frequency is needed. To obtain some numerical estimates, further parameter values are needed. We choose $\overline{n}_3$ in cm$^{-3} = 100$, 400, and 800, respectively; $\sqrt{\langle \delta n_3^2 \rangle} = \overline{n}_3$; and C_n^2 in m$^{-2/3} = 10^{-14}$, 10^{-13}, and 10^{-12}, respectively. The macroscale is estimated at $L_o \sim 25$ m and the average particle diameter at $\overline{D} \sim 5$ μm. These values cover a common range for the relevant parameters. C_n^2 can be influenced significantly by fluctuations in water-vapor density [17]–[19] so that the higher values may account partially for that possibility. Fig. 2 shows plots of the cross sections in (16) as a function of frequency. Each cross section is shown for three different values of the relevant variable parameter [(16) indicates the dependence upon each of these]. Fig. 3 shows plots of $\sigma_{qct} + \sigma_{qcah}$ as a function of frequency and plots of $\sigma_{qct} + \sigma_{qcah} + \sigma_{inc}$ as a function of frequency. In general, results obtained are similar to those of Gossard [17], but are now done for gamma function models of the particle density with only a weak dependence upon the gamma-function power of D.

IV. Doppler Analysis

We now extend the above analysis to Doppler processing of the backscattered pulses, i.e., information on the observed velocity components along the line-of-sight will be used via the concomitant Doppler frequency shifts to produce records of the backscatter amplitudes or powers as a function of the shifted frequency. Several recent studies [19]–[25] have dealt with Doppler processing of radar returns from clouds.

A narrow-band (pulsed) signal $E_o(t) = A_o(t)e^{-i\omega_c t}$ yields, instead of (1), for the backscattered pulse from all the particles in a range cell

$$\begin{aligned} E_{bs}(t) &\approx f_v \sum_m A_o[t - 2R_m(t)/c] e^{-i\omega_c[t - 2R_m(t)/c]} \\ f_v &\equiv \frac{q}{\Gamma\left(\dfrac{p+1}{q}\right)} \int_o^\infty dx x^p e^{-x^q} f_m(D_o x) \end{aligned} \tag{17}$$

where $f_m(\cdots)$ is the backscatter amplitude from a spherical particle with given dielectric permittivity and diameter $D_o x$ and R_m is the range parameter of particle m. A modified gamma function $\propto D^p \exp(-(D/D_o)^q$ has been assumed for the particle-size distribution function $n_4(D)$ and $\Gamma(\cdots)$ is the customary mathematical gamma function. The parameter f_v has a simple dependence upon wavenumber $k = \omega_c/c$ and upon D_o in the Rayleigh regime where $kD_o \ll 1$. Some obvious narrow-band signal approximations are included in the above.

The amplitude autocorrelation is $\mathcal{R}(\tau) \equiv \langle A_{bs}(t) A_{bs}(t+\tau) \rangle$, where the angled brackets indicate averaging over a number of consecutive pulses (with constant τ). Under the assumption of short averaging times such that the motion of $R(t) \approx R + v_m t$ is expected to be linear with time and also [see transition

from (20) to (21)] such that the motion can be neglected in the pulse-envelope amplitude, we find

$$\mathcal{R}(\tau) = |f_v|^2 \left\langle \sum_m \sum_n \langle A_o(t - 2R_m/c) A_o(t + \tau - 2R_n/c) \right\rangle \times e^{2ik_c(R_m - R_n)} e^{-i\Omega_m \tau} \tag{18}$$

with Doppler-shift frequency $\Omega_m \equiv 2k_c v_m$. A transition to continuous notation is effected with $\sum_m \rightarrow \int_{v_{rc}} d^3r' \int_{D_i}^{D_f} dD\, n_4(\vec{r}', D) \int d\Omega s(D, \Omega) \cdots$. Here, $n_4(\vec{r}', D)$ is the particle size distribution at $\vec{r}'$, with dimension (*length*)$^{-4}$, and $s(D, \Omega)$ is a spectral distribution, with dimension (*time*) of Doppler shifts Ω, which are assumed to depend on particle diameter D but not on location $\vec{r}'$. This latter assumption corresponds to homogeneous turbulence in the range cell. We also assume that $n_4(\vec{r}', D) = n_3(\vec{r}')N(D)$, with $N(D)$ implied by (4), so that the zero to ∞ integral of $N(D)$ over D is unity. Hence, in continuous notation we write

$$\begin{aligned}\mathcal{R}(\tau) = |f_v|^2 &\int d^3r' \int d^3r'' \langle n_3(\vec{r}') n_3(\vec{r}'') \rangle e^{2ik_c(z' - z'')} \\ &\times \langle A_o(t - 2z'/c) A_o(t + \tau - 2z''/c) \rangle \\ &\times \int dD N(D) \int d\Omega s(D, \Omega) e^{-i\Omega\tau}. \end{aligned} \tag{19}$$

The Doppler spectrum is obtained by taking the Fourier transform of (19) to obtain $\Phi(\omega)$

$$\begin{aligned}\Phi(\omega) = |f_v|^2 &\int d^3r' \int d^3r'' \langle n_3(\vec{r}') n_3(\vec{r}'') \rangle e^{2ik_c(z' - z'')} \\ &\times \int dD N(D) \int d\Omega s(D, \Omega) \Phi_A(\omega - \Omega)\end{aligned}$$

with

$$\Phi_A(\omega) \equiv \int d\tau \langle A_o(t - 2z'/c) A_o(t + \tau - 2z''/c) \rangle e^{-i\omega\tau}. \tag{20}$$

It is assumed here that the Fourier transform of the pulse amplitude is narrow compared to the width of the spectral density $s(D, \omega)$ so that setting $\tau = 0$ inside the second pulse-amplitude factor in $\Phi_A(\omega)$ would not affect the result significantly. Consequently (20) simplifies to

$$\begin{aligned}\Phi(\omega) = 2\pi|f_v|^2 &\int d^3r' \int d^3r'' \langle n_3(\vec{r}') n_3(\vec{r}'') \rangle e^{2ik_c(z' - z'')} \\ &\times \langle A_o(t - 2z'/c) A_o(t - 2z''/c) \rangle \\ &\times \int dD N(D) s(D, \omega). \end{aligned} \tag{21}$$

The Wiener–Khintchine theorem [26] connecting the Fourier transforms $\mathcal{R}(\tau)$ and $\Phi(\omega)$, implies that $\langle |E_{bs}|^2 \rangle = \mathcal{R}(0) = \frac{1}{2\pi} \int d\omega \Phi(\omega)$, which implies in (4) that

$$\int d\omega \int dD N(D) s(D, \omega) = 1 \tag{22}$$

or, if $s(\omega)$ is not a function of D, that $\int d\omega\, s(\omega) = 1$. Equation (22) also follows as a consequence of comparing (18) and (19) to each other for $\tau = 0$. $\mathcal{R}(0)$ gives the correct result for a sum of incoherent and quasi-coherent scatterers if

$$\langle n_3(\vec{r}') n_3(\vec{r}'') \rangle = \overline{n}_3(z') \delta(\vec{r}' - \vec{r}'') + \langle \delta n_3(\vec{r}') \delta n_3(\vec{r}'') \rangle. \tag{23}$$

Therefore, a similar assumption—with one difference—is introduced into (21), namely

$$\begin{aligned}&\langle n_3(\vec{r}') n_3(\vec{r}'') s(D, \omega) \rangle \\ &\quad = \overline{n}_3(z') s_{inc}(D, \omega) \delta(\vec{r}' - \vec{r}'') \\ &\qquad + \langle \delta n_3(\vec{r}') \delta n_3(\vec{r}'') \rangle s_{qc}(D, \omega). \end{aligned} \tag{24}$$

The two spectral distributions of velocities (Doppler shifts) $s_{inc}(D, \omega)$ and $s_{qc}(D, \omega)$ are allowed to be different as a consequence of which

$$\begin{aligned}\Phi(\omega) &= \Phi_{inc}(\omega) + \Phi_{qc}(\omega) \\ \Phi_{inc}(\omega) &= 2\pi|f_v|^2 \int d^3r' \overline{n}_3(z') A_o^2(t - 2z'/c) \\ &\qquad \times \int dD N(D) s_{inc}(D, \omega) \\ \Phi_{qc}(\omega) &= 2\pi|f_v|^2 \int d^3r' \langle \delta n_3^2(z') \rangle A_o^2(t - 2z'/c) \Phi(2k) \\ &\qquad \times \int dD N(D) s_{qc}(D, \omega). \end{aligned} \tag{25}$$

Consider, finally, that $t = 2z/c$ is the center of a range cell. If that range cell is sufficiently short so that it is statistically uniform, then the integrals are only over squared-pulse amplitudes and thus deliver only the power in one pulse as a factor in each of the spectral functions above. Consequently

$$\begin{aligned}\Phi(\omega) &= \Phi_{inc}(\omega) + \Phi_{qc}(\omega) \quad \text{with} \\ \Phi_{inc}(\omega) &\propto \sigma_{inc} \int dD N(D) s_{inc}(D, \omega) \\ \Phi_{qc}(\omega) &\propto \sigma_{qc} \int dD N(D) s_{qc}(D, \omega) \end{aligned} \tag{26}$$

with identical constants of proportionality. The cross sections σ_{inc} and $\sigma_{qc} = \sigma_{qct} + \sigma_{qcah}$ are defined in (16), but also are easily inferred from (26) above.

V. Hypothetical Velocity Spectrum

In this section, we attempt to discern the type of spectra that can ensue for (16). Consider first the incoherent Doppler spectrum $s_{inc}(D, \omega)$ under the very general assumption that each particle has a velocity $v_m = \overline{v}_m + \delta v_m$ such that $\overline{v}_m(D)$ is an average particle-dependent velocity, and $\delta v_m(D)$ is a fluctuation around the average, possible due to turbulence. In all likelihood, the average velocity is due to gravity with, possibly, some (vertical) wind component in addition. A simple assumption for the incoherent Doppler spectrum restricted in form largely for mathematical tractability is

$$s_{inc}(D, \omega) = \tau(D)\, e^{-[\omega - \overline{\omega}(D)]^2 / 2\sigma^2(D)} \tag{27}$$

implying a Gaussian velocity spread around an average velocity that depends only on particle diameter D (and not on position), and determined also by D-dependent parameters. The $\tau(D)$ is

a normalization parameter. We make some additional assumptions for mathematical tractability. Let $\overline{\omega}(D) = \omega_o(D/D_o) \equiv \omega_o\xi$ with constant frequency ω_o and normalized diameter $\xi = D/D_o$. This amounts to an assumption that the average single-particle velocity is proportional to the particle diameter. While this is approximately true only for a limited range of diameters [6], [27], it allows us to proceed because then we also can assume (for simplicity) that $\sigma(D) \equiv \sigma$ is small enough so that the Gaussian can be approximated by a delta function with

$$e^{-[\omega-\overline{\omega}(D)]^2/2\sigma^2(D)} \to \delta[\omega-\overline{\omega}(D)] = \frac{1}{\omega_o}\,\delta(\xi-\omega/\omega_o)$$
$$N(D)\,dD = \frac{q}{\Gamma\left(\dfrac{p+1}{q}\right)}\xi^p\,e^{-\xi^q}\,d\xi. \tag{28}$$

This latter simplification is not essential and calculations can be made directly with the Gaussian form. But if this simplification is made, then

$$\Phi_{inc}(\omega) \propto \sigma_{inc}\,\frac{1}{\omega_o}\,\frac{q}{\Gamma\left(\dfrac{p+1}{q}\right)}\int_0^\infty d\xi\xi^p e^{-\xi^q}\delta(\xi-\omega/\omega_o) \tag{29a}$$

which is properly normalized so that we can choose $\tau(D) = 1$ in (27). Equation (29a) is easily expressed in a new dimensionless frequency variable $\Omega = \omega/\omega_o$ as

$$\Phi_{inc}(\omega) \propto \sigma_{inc}\,\frac{1}{\omega_o}\,\frac{q}{\Gamma\left(\dfrac{p+1}{q}\right)}\Omega^p e^{-\Omega^q}. \tag{29b}$$

Typical cloud distributions with particle sizes up to perhaps 50 μm can be modeled by gamma distributions with $4 < p < 6$ and $q = 1$ so that, e.g., for $p = 6$

$$\Phi_{inc}(\omega) \propto \sigma_{inc}\,\frac{1}{\omega_o}\,\frac{1}{720}\,\Omega^6 e^{-\Omega}. \tag{30}$$

Next, consider the quasi-coherent Doppler spectrum $s_{qct}(D, \omega)$ under the assumption that each "turbule" has a velocity $v_m = \overline{v}_m + \delta v_m$ such that $\overline{v}_m(D) \approx 0$ is a (negligible) average velocity and δv_m is a fluctuation around the average, which we shall assume to be particle-diameter independent as the particles are convected by the underlying turbulent fluctuations in wind velocity. One simple assumption for the quasi-coherent Doppler spectrum is

$$s_{qc}(D, \omega) = \frac{\sqrt{2\pi}}{\omega_{qc}}\,e^{-\omega^2/2\omega_{qc}^2} \tag{31}$$

which is properly normalized and introduces a new frequency parameter ω_{qc}. This then yields

$$\Phi_{qc}(\omega) \propto \sigma_{qc}\,\frac{\sqrt{2\pi}}{\omega_{qc}}\,e^{-\omega^2/2\omega_{qc}^2} = \sigma_{qc}\alpha\,\frac{\sqrt{2\pi}}{\omega_o}\,e^{-\alpha^2\Omega^2} \tag{32}$$

with $\alpha = \omega_o/\omega_{qc}$ expressing the ratio between the two frequency parameters. The final result is

$$\Phi(\omega) = \Phi_{inc}(\omega) + \Phi_{qc}(\omega)$$
$$= \frac{\sigma_{inc}}{720}\left[\Omega^6\,e^{-\Omega} + 720\sqrt{2\pi}\alpha\,\frac{\sigma_{qc}}{\sigma_{inc}}\,e^{-(\alpha\Omega)^2}\right]. \tag{33}$$

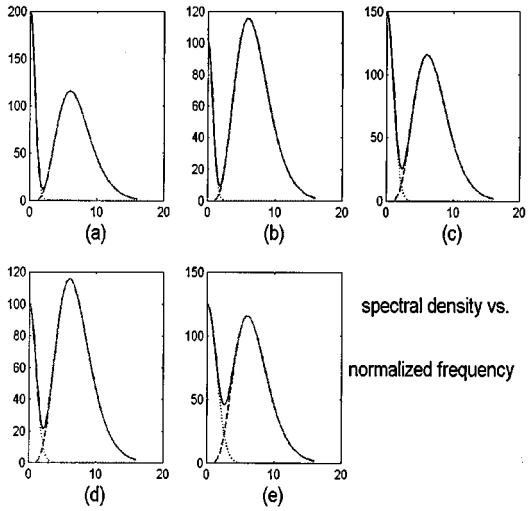

Fig. 4. Doppler spectral density $\Phi(\omega)$ versus normalized frequency $\Omega = \omega/\omega_o$ [see (34)]—$\Phi(\Omega)$ = solid line $\Phi_{inc}(\omega)$ = dashed line $\kappa\alpha\Phi_{qc}(\omega)$ = dotted line. (a) $\kappa = 200$, $\alpha = 1$. (b) $\kappa = 100$, $\alpha = 1$. (c) $\kappa = 300$, $\alpha = 0.5$. (d) $\kappa = 200$, $\alpha = 0.5$. (e) $\kappa = 500$, $\alpha = 0.25$.

In order to obtain some idea of the spectrum, let us write (33) as follows:

$$\Phi(\omega) = \Omega^6\,e^{-\Omega} + \kappa\alpha\,e^{-(\alpha\Omega)^2} \tag{34}$$

so that κ represents $720\sqrt{2\pi}\sigma_{qc}/\sigma_{inc}$.

Fig. 4(a)–(e) depict graphs of normalized spectral density $\Phi(\omega)$ versus normalized frequency $\Omega = \omega/\omega_o$ for various values of κ and α. To put these values in perspective: $720\sqrt{2\pi} \approx 1805$ so that $k = 300$ implies that $\sigma_{qc}/\sigma_{inc} \approx 1/6$. As stated above, $\alpha = \omega_o/\omega_{qc}$. These graphs show a double-humped spectrum with a peak at $\Omega = 0$ due to turbulence, and a peak at some $\Omega > 0$ due to the individual incoherent velocity spectrum. The chosen model places that peak at $\Omega = 6$, but that is only an artifact of this particular model. Sizable deviations of α or κ from the given values can result in sum spectra that are not bimodal. Larger values of α give deeper dips between peaks, and larger values of κ increase the first peak with respect to the second.

It is shown in this section that the occurrence of radar reflections from turbulently convected cloud droplets can give rise to a Doppler spectrum with peaks at zero and at a distinct nonzero frequency. The magnitude of each portion of the spectrum, as well as the location of the maxima, are functions of the number density, the velocity parameters, the strength of turbulence, as well as the operating frequency. In this study, it has been assumed that the root mean square (rms) density $\delta n_{\rm rms}$ is the same as the average $\overline{n}$, but the results are changed for lower values of $\delta n_{\rm rms}/\overline{n}$ only in that the values of κ are changed proportionately in obtaining similar graphs. However, other mechanisms not accounted for here also may contribute to the observed types of Doppler spectra. For example, a few ice or snow particles, with very different velocity distributions, may contribute strongly to the reflections because the reflected power from a small particle is proportional to the sixth power of diameter and such particles are generally much larger than the micron water droplets in clouds. Resolution awaits further experimental evidence.

REFERENCES

[1] H. C. van de Hulst, *Light Scattering By Small Particles*. New York: Wiley, 1957.

[2] C. F. Bohren and D. R. Huffman, *Absorption And Scattering Of Light By Small Particles*. New York: Wiley, 1983.

[3] L. Tsang, J. A. Kong, and R. T. Shin, *Theory of Microwave Remote Sensing*. New York: Wiley, 1985.

[4] 22151V. I. Tatarskii, "The effects of the turbulent atmosphere on wave propagation," Nat. Tech. Inform. Service, U.S. Dept. Commerce, Springfield, VA, Document TT 68-50464, 1971.

[5] A. Ishimaru, *Wave Propagation And Scattering In Random Media—Vol. I, II*. New York: Academic, 1978.

[6] R. J. Doviak and D. S. Zrnić, *Doppler Radar and Weather Observations*, 2nd ed. San Diego: Academic, 1993.

[7] H. R. Pruppacher and J. D. Klett, *Microphysics of Clouds and Precipitation*. Dordrecht, The Netherlands: D. Reidel, 1978.

[8] L. P. Ligthart and L. R. Nieuwkerk, "Studies of precipitation processes in the troposphere using an FM-CW radar," *J. Atmosph. Ocean. Technol.*, vol. 6, pp. 798–808, 1989.

[9] D. A. de Wolf and C. Kontogeorgakis, "Reflectivity and attenuation at millimeter to infrared wavelengths for advection fogs at four locations," *J. Appl. Meteorol.*, vol. 38, pp. 126–131, Jan. 1999.

[10] J. Allen Zak, "Drop size distributions and related properties of fog for five locations measured from aircraft,", NASA Contractor Rep. 4585 (DOT/FAA/CT-94/02), April 1994.

[11] S. A. Smith and P. R. Jonas, "Observations of turbulence in cirrus clouds ," *Atmospheric Research*, vol. 43, pp. 1–29, Nov. 1996.

[12] I. Gultepe and D. O. Starr, "Dynamical structure and turbulence in cirrus clouds: Aircraft observations during FIRE," *J. Atmos. Sci.*, vol. 52, pp. 4159–4418, Dec. 1995.

[13] H. G. Booker and W. E. Gordon, "A theory of radio scattering in the troposphere," *Proc. IRE*, vol. 38, pp. 401–412, 1950.

[14] F. Villars and V. F. Weisskopf, "On the scattering of radio waves by turbulent fluctuations in the atmosphere," *Proc. IEEE*, vol. 43, pp. 1232–1239, 1955.

[15] C. C. Lin, *Statistical Theories of Turbulence*. Princeton, NJ: Princeton Univ. Press, 1961.

[16] E. E. Gossard and R. G. Strauch, "The refractive index spectra within clouds from forward-scatter radar observations," *J. Appl. Meteor.*, vol. 20, pp. 170–183, 1981.

[17] E. E. Gossard, "A fresh look at the radar reflectivity of clouds," *Radio Sci.*, vol. 14, pp. 1089–1097, 1979.

[18] U. Merlo, E. Fionda, and J. Wang, "Ground level refractivity and scintillation in space-earth links," *Appl. Opt.*, vol. 27, pp. 2247–2252, 1988.

[19] N. I. Fox and A. J. Illingworth, "The retrieval of stratocumulus cloud properties by ground based cloud radar," *J. Appl. Meteorol.*, vol. 36, pp. 485–492, May 1997.

[20] V. C. Chen, "Applications of the time frequency processing to radar imaging," *Opt. Eng.*, vol. 36, pp. 1152–1161, Apr. 1997.

[21] E. E. Gossard, J. B. Snider, E. E. Clothiaux, B. Martner, J. S. Gibson, R. A. Kropfli, and A. S. Frisch, "The potential of 8 mm radars for remotely sensing cloud drop size distributions," *J. Atmosph. Ocean. Technol.*, vol. 14, pp. 76–87, Feb. 1997.

[22] F. M. Ralph, P. J. Neiman, D. W. VandeKamp, and D. C. Law, "Using spectral moment data from NOAA 404 MHz radar wind profilers to observe precipitation," *Bull. Amer. Meteorolog. Soc.*, vol. 76, pp. 1717–1739, Oct. 1995.

[23] A. S. Frisch, C. W. Fairall, and J. B. Snider, "Measurement of stratus cloud and drizzle parameters in ASTER with a K Alpha band Doppler radio and a microwave radiometer," *J. Atmosph. Sci.*, vol. 52, pp. 2788–2799, Aug. 1995.

[24] G. M. Barnes, "Updraft evolution: A perspective from cloud base," *Monthly Weather Rev.*, vol. 123, pp. 2693–2715, Sep. 1995.

[25] F. M. Ralph, "Using radar measured radial vertical velocities to distinguish precipitation scattering from clear air scattering," *J. Atmosph. Ocean. Technol.*, vol. 12, pp. 257–267, Apr. 1995.

[26] A. M. Yaglom, *An Introduction to the Theory of Stationary Random Functions*. New York: Dover, 1962. (trans. by R. A. Silverman).

[27] A. Deepak, Ed., *Atmospheric Aerosols : Their Formation, Optical Properties, and Effects*. Hampton, VA: Spectrum, 1982.

David A. de Wolf received the B.Sc. degree in physics and mathematics and the Dutch Doctorandus degree in theoretical physics, both from the University of Amsterdam, the Netherlands, in 1955 and 1959, respectively, and the Doctorate degree in technology from TU Eindhoven, The Netherlands, in 1968.

From 1962 to 1982, he was with RCA Laboratories, David Sarnoff Research Center, Princeton, NJ, where his earlier work covered various aspects of radio-, radar-wave, and optical scattering from atmospheric media and objects, and also wave propagation through irregular media. Subsequently, he worked on electron-optics applications to TV systems, specifically with respect to guiding electron beams accurately in complicated electromagnetic fields. In 1982 he joined the Electrical Engineering Department, Virginia Tech, Blacksburg. Since then he has worked on problems concerning scattering in particulate media, especially regarding propagation of radar and optical waves through rain, fog, haze, and other aerosols. He has been associated in the summers with TU Delft's International Research Centre for Telecommunications-Transmission and Radar (and predecessor organizations) since 1988. He is the author of a text on electron optics and of a forthcoming undergraduate text on electromagnetic theory.

Dr. de Wolf is a Fellow of the Optical Society of America and a member of the American Association of Physics Teachers, the Dutch Physical Society, Sigma Xi, and Eta Kappa Nu, as well as Commissions B and F of the USNC of the International Union of Radio Science.

Herman W. J. Russchenberg, photograph and biography not available at time of publication.

Leo P. Ligthart, photograph and biography not available at time of publication.